The systems biology of MHC class II antigen presentation
Paul, P.

Cover Page

Universiteit Leiden

The handle http://hdl.handle.net/1887/19743 holds various files of this Leiden University dissertation.

Author: Paul, Petra
Title: The systems biology of MHC class II antigen presentation
Date: 2012-09-06

Chapter 1

A Genome-wide Multi-Dimensional RNAi Screen Reveals Pathways Controlling MHC Class II Antigen Presentation

Petra Paul*, Tineke van den Hoorn*, Marlieke L.M. Jongsma*, Mark J. Bakker, Rutger Hengeveld, Lennert Janssen, Peter Cresswell, David A. Egan, Marieke van Ham, Anja ten Brinke, Huib Ovaa, Roderick L. Beijersbergen, Coenraad Kuijl and Jacques Neefjes

* equal contribution

The Antigenic Peptide

The MHC Class II α-chain

The MHC Class II β-chain
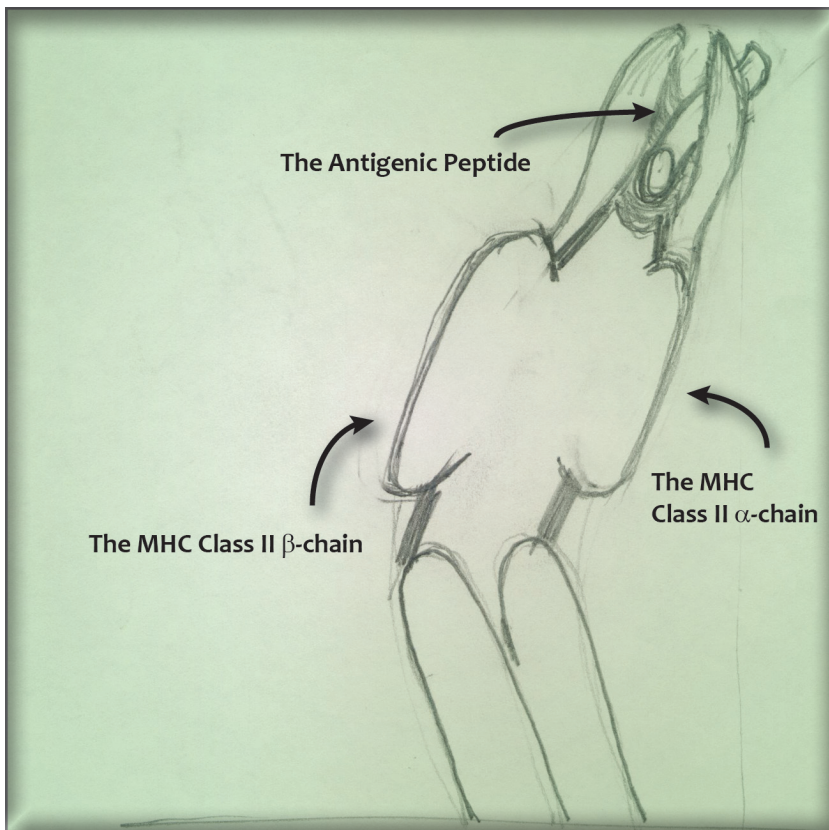
MHC class II molecules (MHC-II) present peptides to T helper cells to facilitate immune responses and are strongly linked to autoimmune diseases. To unravel processes controlling MHC-II antigen presentation, we performed a genome-wide flow cytometry-based RNAi screen detecting MHC-II expression and peptide loading followed by additional high-throughput assays. All datasets were integrated to answer two fundamental questions: what regulates tissue-specific MHC-II transcription and what controls MHC-II transport in dendritic cells. MHC-II transcription was controlled by nine regulators acting in feedback networks with higher order control by signalling pathways including TGFβ. MHC-II transport was controlled by the GTPase ARL14/ARF7, which recruits the motor myosin 1E via an effector protein ARF7EP. This complex controls movement of MHC-II vesicles along the actin cytoskeleton in human dendritic cells (DCs). These genome-wide systems analyses have thus identified factors and pathways controlling MHC-II transcription and transport, defining targets for manipulation of MHC-II antigen presentation in infection and autoimmunity.

Introduction

Major Histocompatibility Complex class II molecules (MHC-II) present peptides to CD4$^+$ T cells that initiate and control immune responses. The expression of MHC-II is mostly restricted to professional antigen presenting cells (APCs), such as B cells and dendritic cells (DCs), and controlled by a transcriptional complex that includes the MHC-II transactivator CIITA [1]. Careful regulation of expression is needed to prevent uncontrolled immune responses. Various allelic forms of MHC-II are associated with autoimmune diseases [2]. The successful presentation of peptides at the cell surface involves a series of subcellular events: In the ER, MHC-II associates with the invariant chain (Ii) that fills the peptide-binding groove and mediates transport to late endosomal compartments called MHC-II compartments (MIICs) [3, 4]. There, Ii is degraded leaving a fragment called CLIP in the peptide-binding groove of MHC-II [5]. In parallel, endocytosed antigens are degraded into peptides, which compete with CLIP for binding to MHC-II in a process catalyzed by the chaperone HLA-DM (DM) [6, 7] in the intraluminal vesicles of the MIIC [8]. Ultimately, MHC-II-containing vesicles and tubules fuse with the plasma membrane [9-11] to present the peptide-loaded MHC-II to CD4$^+$ T cells.

Various factors controlling MHC-II expression have been identified, such as cytokines that can inhibit (IL-10) [12] or upregulate (interferon-γ) [13] MHC-II

expression. Certain activation signals, such as TLR signalling can also upregulate its expression in B cells and DCs [14]. IL-10 signalling may upregulate MARCH I, which ubiquitinates and shortens MHC-II half-life [15]. Other factors such as pH [16], kinases [17] and cholesterol [18] affect MHC-II expression and antigen presentation.

As a first step towards a systems-understanding of MHC-II antigen presentation, we performed a multi-dimensional RNAi screen where we investigated cell surface expression of MHC-II, as well as peptide loading, transcriptional control and intracellular distribution in an integrated manner. Combining these phenotypic analyses yielded factors and pathways controlling MHC-II transcription and transport in DCs and defined targets for manipulation of MHC-II antigen presentation in infection and autoimmunity.

Results

Genome-wide RNAi Screen identifies 276 Candidate Genes affecting MHC-II Expression and Peptide Loading

MHC-II is selectively expressed by APCs. To identify proteins and networks involved in MHC-II expression and peptide loading, we selected the human melanoma cell line MelJuSo, which expresses peptide-loaded MHC-II and all components required for MHC-II antigen presentation [11]. Whereas MelJuSo is not an immune cell type, it does express many immune-specific genes and proteins controlling MHC-II transport similar to DCs. APCs express Toll-like receptors (TLRs) recognizing double-stranded siRNA resulting in activation signals that might increase MHC-II expression [19, 20]. MelJuSo lacks these TLRs and in addition exhibits transfection efficiencies greater than 95%, as well as stable MHC-II expression and peptide loading capacity (data not shown). These features, which are essential for reliable RNAi screens, are not shared by any primary APC tested.

To visualize the effects of gene knockdown on MHC-II expression and peptide loading, we used two monoclonal antibodies (Figure 1A). Cy5-conjugated CerCLIP, which recognizes human MHC-II loaded with the residual Ii-derived CLIP fragment, and Cy3-conjugated L243, which recognizes peptide-loaded MHC-II (called HLA-DR). CLIP-loaded MHC-II reflects an inefficiency of the loading of antigenic peptide on the mature receptor [21], whereas L243 detects correctly loaded MHC-II on the plasma membrane [22]. MelJuSo cells were transfected with pools of siRNAs (four duplexes per target gene) in 96-well format targeting 21,245 human genes in total. Three days post-transfection, cells were analyzed by flow

LIBRARIES

LIBRARIES	Targets
Kinome	780
DUB	128
Drugome	6,022
GPCR	515
Rest of human genome	13,800

RNAinterference

Human Genome	Primary Screen	Rescreen	Microarray	Deconvolution
21.245 Targets	961 Targets with CerCLIP or L243 effect	789 Targets confirmed	532 Targets expressed in Immune Cells	276 Targets confirmed (>2 Duplexes)

		Effect	#
A	L243	up	105
B	L243	down	18
C	CerCLIP	up	44
D	L243 / CerCLIP	up	109
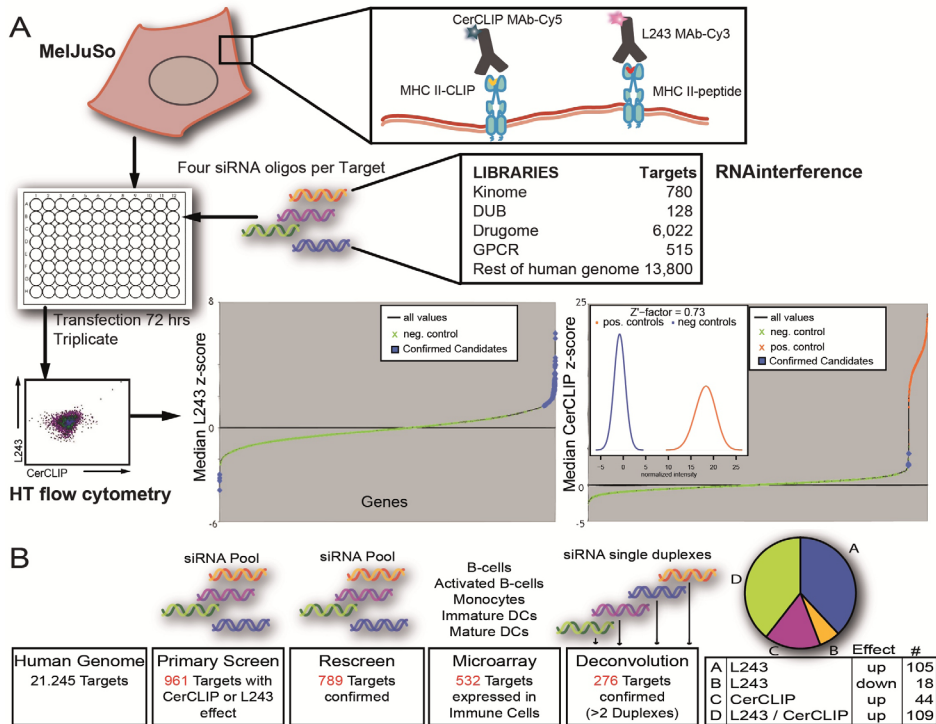
Figure 1 | A genome-wide Flow Cytometry-based RNAi Screen

A | MelJuSo transfected with siRNA were analysed for surface expression of peptide- versus CLIP-loaded MHC-II by high-throughput flow cytometry using monoclonal antibodies (L243-Cy3 and CerCLIP-Cy5). The graphs show representative z-scores of siRNAs without effect ($|z|<3$; black line), untreated cells (green), HLA-DM-silencing (orange) and candidates after normalization ($|z|>3$; blue). Inlay in the CerCLIP plot shows the Z'-factor for the analysis of the kinase sublibrary, representing the detection window between negative (blue) and positive controls (red).

B | Scheme showing the different confirmation steps in the screening procedure resulting in 276 candidate genes influencing MHC-II expression and peptide loading. Indicated is the distribution of four phenotypes detected by flow cytometry. See also Table S1 and S2 in Chapter 2 of this thesis.

cytometry to determine peptide loading as well as expression levels of MHC-II. The primary screen (performed in triplicate) achieved an excellent "screening window" (difference of negative and positive control) defined by the Z' factor [23]. All parts yielded Z'>0.5 (Figure 1A; Z' for the kinase sub-library). Results were z-score normalized. Genes whose silencing resulted in a change of L243 or CerCLIP staining by $|z|>3$ (p<0.0027) were considered candidates for follow up. These genes were re-screened in triplicate, resulting in 789 candidate proteins with potential functions in controlling MHC-II expression and peptide loading (Figure 1B).

To determine which of the 789 candidates identified in the screen were expressed in APCs, we performed microarray gene expression analysis on human primary monocytes, monocyte-derived (activated and immature) DCs and naïve or CD40L-activated B cells (Table S1, see Chapter 2 of this thesis). Of the candidate genes identified in MelJuSo cells, 532 genes were expressed in one or more human primary APC type. Correcting for off-target effects (see Experimental Procedures) resulted in 276 confirmed candidates (Table S2, see Chapter 2 of this thesis). These candidates could be divided into four groups based on differential staining with L243 or CerCLIP, which allowed the distinction between effects on MHC-II expression versus effects on peptide loading, respectively. Most candidate proteins identified in the screen appeared to affect MHC-II surface expression; only 45 genes specifically affected peptide loading (CLIP up; Figure 1B).

Candidate Proteins include known MHC-II Pathway Components and Proteins associated with Autoimmunity

To annotate the function of the 276 identified genes, we used database tools to determine tissue distribution, potential function, association with autoimmune diseases and established function in the MHC-II antigen presentation pathway. First, as a validation of our method, we interrogated the dataset for proteins already known to be involved in MHC-II antigen presentation. Thirteen candidates have been reported in literature to control MHC-II antigen presentation (Figure 2A, green/yellow proteins), including the MHC-II transcriptional regulator CIITA, the HLA-DRA and DRB chains, DM and the IL-10 receptor. Another set of 13 proteins might indirectly correlate to the pathway through inhibitors or as targets of pathogenic immune regulators (Figure 2A, blue proteins). For example, FKBP3 (FK506-binding protein 3) may be the target of FK506 [24]. The target(s) for general kinase inhibitor Staurosporine [17] can be included in the 28 serine/threonine kinases we identified in our screen. Also, the immunodeficiency virus (HIV) protein Tat has been postulated to control HIV-Tat Interacting Protein (HTATIP) [25] (Figure 2A), which we picked up in our screen as a regulator of MHC-II peptide loading. Hence, some 10% (26 of 276) of our primary screen candidates have already been implicated in controlling MHC-II expression and peptide loading. In our initial screen however, we did not identify all factors that had been reported in literature to control MHC-II function. We thus retested these separately, which revealed that most of them yielded effects below our cut-off of |z|>3 (Figure S1, see Chapter 2 of this thesis).

Second, to determine which candidate genes were selectively expressed in immune tissues, we interrogated a gene expression database of 79 human tissues [26], and compared expression levels of each candidate between immune and other tissues. The expression of CIITA is limited to antigen presenting cells, therefore we used its expression as a standard for immune-specificity (Figure 2B). Sixty-nine of the 276 candidates identified by the RNAi screen exhibited selective expression in immune tissues (Table S1, see Chapter 2 of this thesis).

Another interesting group in which some of our candidates could be placed were associated with autoimmunity. Genetic association studies have revealed that MHC-II is the strongest autoimmunity-associated factor [2] possibly triggering the immune response by presenting autoantigens. Comparing our candidates involved in MHC-II regulation with a database containing genes linked to autoimmune diseases (http://geneticassociationdb.nih.gov)

showed that 8% (21 of 276) were associated with autoimmune diseases (Figure 2C). This association, together with their immune tissue-specific expression pattern, makes some of them attractive therapeutic targets for manipulating MHC-II function.

A standard protocol in genome-wide screening is pathway analysis based on literature. We first subclustered candidates into four groups based on their flow cytometry parameters (Figure 1B) before functional annotation by Ingenuity Pathway Analysis (www.ingenuity.com, Figure 2D; Table S2, see Chapter 2 of this thesis). Many enzyme classes are found to be involved in MHC-II antigen presentation, but the majority of genes had no ascribed function. The four groups were then analyzed by Ingenuity Pathways Analysis and STRING [27] for established protein interactions and yielded several networks consisting of annotated proteins only (Figure S2, see Chapter 2 of this thesis). Analysis of these networks revealed clusters of proteins already known to be involved in MHC-II antigen presentation. No novel clusters regulating MHC-II became apparent from this network analysis. As most proteins had unknown functions, these pathways only covered a small fraction of candidate proteins. Hence, network analysis using different database tools was unsatisfactory in terms of describing the systems biology of MHC-II antigen presentation.

Therefore, we aimed at placing candidates in functional networks following secondary high-throughput screens. We broke down MHC-II antigen presentation in three processes: peptide loading (1), transcriptional regulation (2), and the general cell biology of MHC-II (3). The latter category consists of the assembly, intracellular transport, processing in the MIIC, endo- and exocytosis. Factors affecting peptide loading (1) were already identified by the antibody CerCLIP in the primary screen.

After genome-wide screening we were able to confirm our strategy by identifying known members of the MHC-II pathway. Furthermore, we have highlighted interesting therapy targets displaying immune-tissue specific expression and association to autoimmune diseases. Secondary high-throughput assays are needed to decipher the candidates involved in the transcriptional regulation and general cell biology of MHC-II.

Nine Candidates are implicated in Transcriptional and Higher Order Control of MHC-II Expression

MHC-II mRNA expression is controlled by CIITA. To determine whether the 276 candidate genes identified in the earlier RNAi screen affected MHC-II transcription, we silenced the 276 candidates in

Figure 2 | Candidate Gene Annotation

A | A literature-based model representing proteins directly (yellow) and indirectly (blue) involved in the MHC-II pathway (green). See also Figure S1 in Chapter 2 of this thesis. EE = Early Endosome; MIIC = MHC class II containing Compartment; Ii = invariant chain

B | Gene expression ratios of the candidate genes in the primary human immune cells (1) used in our selection procedure (Figure 1B) and immune tissues (2) versus non-immune tissues (3). Grey areas indicate absence of probes on the expression arrays. Expression levels of (2) and (3) were obtained from the BioGPS application.

C | Genes from the screen that are associated to autoimmune diseases based on the Genetic Association Database.

D | Functional annotation of the candidate genes involved in the various effects on MHC-II antigen presentation. Annotation retrieved from Ingenuity Pathways Analysis.

See also Figure S2 and Table S1 and S2 in Chapter 2 of this thesis.

24

MelJuSo cells and performed quantitative PCR for mRNA of MHC-II (HLA-DRA), CIITA, and Ii. To check whether the candidates from our screen controlled the entire MHC locus, MHC class I transcription (HLA-A/B/C) was assessed [28].

The silencing of nine candidate proteins affected transcription of one or several of the tested genes (Figure 3A, Table S3, see Chapter 2 of this thesis). Silencing of three candidate genes (CIITA itself, RMND5B and PLEKHA4) down-regulated CIITA and HLA-DR mRNA levels: The protein RMND5B has an unknown function and PLEKHA4 has so far only been described as a phosphoinositide binding protein. The silencing of three other genes (KIAA1007 [CNOT1], CDCA3 and MAPK1) up-regulated both CIITA and HLA-DR transcription. CNOT1 is part of a transcription regulatory complex called CCR4-NOT. This complex contains also another protein identified in our primary screen, called CNOT2. MAPK1, is a key signalling intermediate in many well-studied pathways and the function of CDCA3 is yet unknown. MAPK1 (and CIITA itself) were the only genes shown to affect the whole MHC-locus, as measured by MHC class I (MHC-I) expression.

Knockdown of unknown EFHD2 and HTATIP increased the expression levels of HLA-DR and Ii. Silencing of only one gene (IL27RA, the IL-27 receptor) affected MHC-I expression independently of CIITA. This probably represents a more locus-specific effect. IL-27RA has been implicated in Th1-type as well as innate immune responses. For a full description of the candidates that affect MHC-II transcription see Table S3 in Chapter 2 of this thesis. These nine candidate genes, including CNOT2, can affect each other's expression as well as that of CIITA, HLA-DR, Ii and MHC-I. To define potential interconnections, we performed a 'cross-correlative qPCR': Each candidate was silenced and the effect on expression of the other candidates was determined by qPCR (Figure 3B). Most siRNAs affected the expression of one or more other candidate genes, suggesting that they act in complex networks (Figure 3C). These networks can be either defined as controlling the CIITA expression (network 1), the MHC locus (network 2) or the selective transcription of HLA-DR and Ii (group 3).

We performed literature analysis to define higher order regulation of the transcriptional network controlling MHC-II expression. Seven of the candidates affecting MHC-II transcription have already been annotated to pathways. FLJ22318/RMND5B (human homologue of yeast Required for Meiotic Nuclear Division 5B protein), on the other hand, is not functionally annotated, but an interaction with SMAD4 has been reported [29]. SMAD-proteins transduce signals from the TGFβ receptor to the nucleus to downregulate MHC-

II expression [30]. To understand the role of this unknown factor, we tested whether RMND5B is involved in TGFβ signaling. Following exposure to TGFβ for three days, MHC-II was downregulated in MelJuSo. RMND5B silencing further downregulated MHC-II expression as detected by flow cytometry and qPCR (Figure 3D, E). RMND5B might thus act as an inhibitor of SMADs. SMAD4 translocates from cytosol to nucleus upon TGFβ exposure [31], which was also observed for RMND5B in MelJuSo (Figure 3F). Although we failed to show a direct interaction with SMAD4, we placed RMND5B in a network controlled by TGFβ signaling, which controls MHC-II expression.

We have defined a transcriptional network controlling MHC-II expression. Furthermore, we described a network of higher order control based on proteins annotated in literature (Figure 3G; for references Figure S3 in Chapter 2 of this thesis). These networks should in principle explain the immune tissue-selective expression of MHC-II. The data show that CIITA expression is controlled by a complex transcriptional feedback mechanism, which in turn is controlled by a series of general biological processes such as chromatin modification, the cell cycle and a number of different signaling events including those mediated by TGFβ and RMND5B. The combined input of events presumably determines the tissue selectivity of MHC-II expression.

Analysis of Networks with similar intracellular MHC-II Distribution Phenotypes selects Candidates for in-depth Study

Nine candidate genes were shown to control the transcription of MHC-II. This implies that the other 268 candidates could affect the intracellular distribution of MHC-II. This we evaluated by microscopy. A clonal MelJuSo cell line expressing MHC-II-GFP and mCherry-GalT2 (a Golgi marker) was transfected with siRNAs for the candidates. The nuclei (Hoechst) and early endosomes (anti-EEA1) were stained to detect all relevant intracellular compartments of MHC-II (Figure 4A and S4A, see Chapter 2 of this thesis). The resulting images were processed with CellProfiler software [32], which resulted in more than 100 parameters describing the features of nuclei, endosomes, Golgi and plasma membrane. Images were analyzed and scored using automated image analysis software (CPAnalyst2; see Supplemental Experimental Procedures for analysis parameters in Chapter 2 of this thesis) [33]. Particular phenotypes could be characterised in this manner: e.g. enlarged MHC-II positive vesicles, MHC-II redistribution to the plasma membrane, clustering or dispersion of early endosomes, and
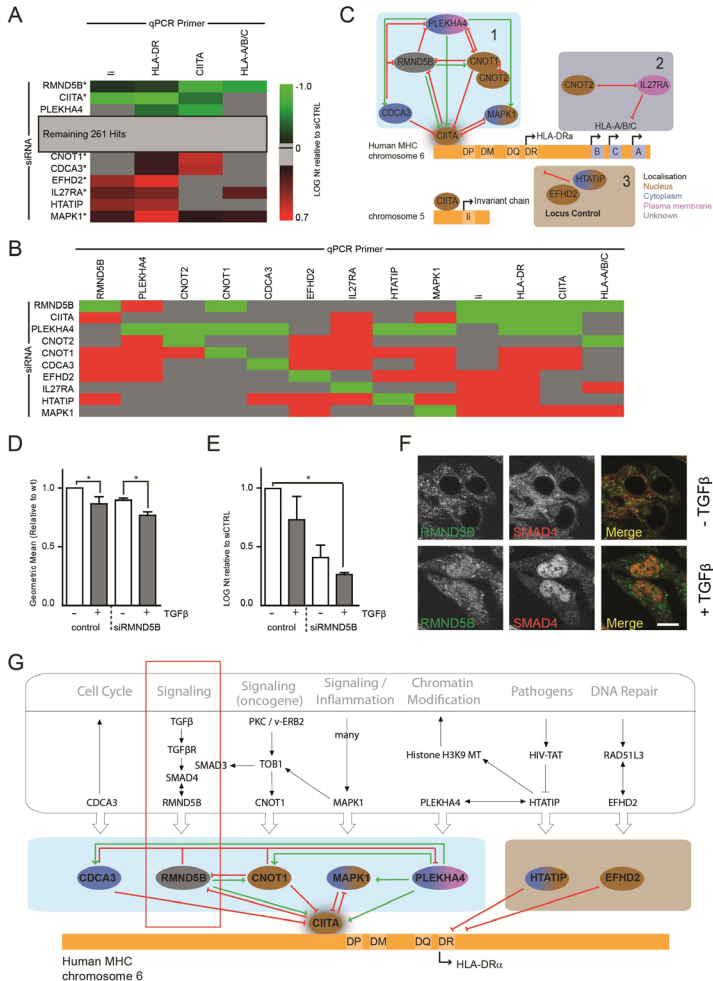
Figure 3 | MHC-II Transcription Control Networks and higher Order Control

A | The heatmap shows the log-transformed expression values (GAPDH as reference) relative to siControl-treated cells (FLJ22318 = RMND5B; KIAA1007 = CNOT1). Mean values of four independent experiments are shown. Stars show correlation between L243 phenotype (Table S2, in Chapter 2 of this thesis) and qPCR.

B | Upon silencing the genes defined under (A), the effect on the expression levels of the nine genes and the MHC-II factors were determined by qPCR. Confirmed effects of at least two experiments are shown (green = down-; red = up-regulation; gray = no effect).

C | Transcriptional networks deduced from the qPCR data controlling CIITA (1), the MHC locus (2) or MHC-II and Ii expression without CIITA involvement (3). Intracellular localisation of the proteins is represented in different colours. Red arrows: inhibition, green arrows: activation of transcription.

D | MHC-II expression on RMND5B silenced MelJuSo cells in presence or absence of TGFβ. Mean fluorescence intensity of three experiments plus standard deviation normalized to control siRNA conditions is plotted. * p<0.05

E | RNA levels of HLA-DR upon RMND5B silencing and TGFβ treatment. LOG-transformed expression levels (relative to GAPDH) from two experiments normalized to control siRNA conditions plus standard deviation are plotted. *p<0.05

F | Intracellular distribution of RMND5B and SMAD4 in MelJuSo in the presence or absence of TGFβ. (bar = 10 mm)

G | Higher order control of the transcriptional network, based on literature and experimental data (red box).

See also Figure S3 and Table S3 in Chapter 2 of this thesis.
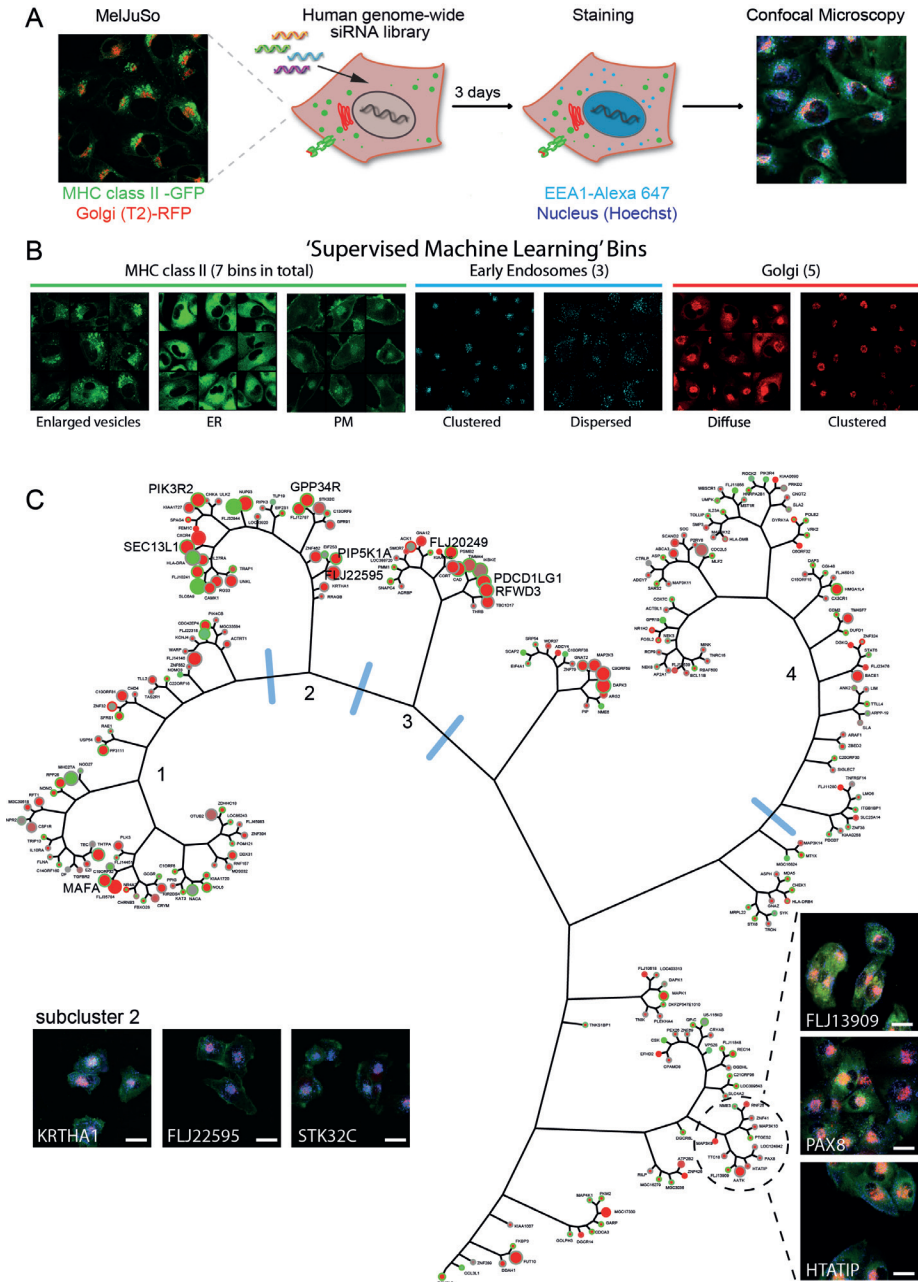
Figure 4 | MHC-II Distribution Control: Automated Image Analysis

A | MelJuSo stably expressing MHC-II (HLA-DRB1-GFP, green) and a Golgi marker (mCherry-GalT2, red) were transfected with siRNA targeting the 276 candidate genes and stained for early endosomes (EEA1) in blue and nucleus (Hoechst, not shown).

B | Confocal images of all silenced genes were analysed using CellProfiler and CPAnalyst 2. In the process of 'supervised machine learning', siRNAs resulting in similar phenotypes were manually grouped into several bins for the different fluorescent channels. Shown are panels with representative images used for computer instruction. The minimal number of descriptive parameters for each group was determined.

Figure 4 | continued

C | Organic view of clustered genes based on phenotype determined by quantitative microscopy analysis. The color of the nodes indicates the z-score for the L243 staining (red: up-, green: down-regulation). The nodes' border color indicates the change in mRNA levels upon DC maturation (red: higher, green: lower expression). Node size represents a measure of mDC phenotype. A larger node is correlated to higher cell membrane MHC-II levels related to intracellular vesicles. Names in large font indicate selected candidates for further testing in DCs. Example images of genes from selected clusters are shown. (bar = 25 mm)

See also Figure S4 and S5, Table S4 in Chapter 2 of this thesis.

---

altered Golgi structure (Figure 4B). After several rounds of software training, the minimal number of parameters (out of the >100) needed to distinguish the phenotypes was determined (Figure S4B and Table S4, see Chapter 2 of this thesis). After z-score normalization, the siRNAs giving similar phenotypes were clustered (Figure 4C). Control siRNAs (positive and non-affecting) were clustered in distinct groups, thereby validating our method.

To obtain an overview of our data, we built a network tree integrating information of all the different screens. The fill-color of each gene shows the effect on MHC-II surface expression (L243, flow cytometry screen), while the color of the edge represents mRNA level changes going from immature (im)DCs to mature (m)DCs, as found by microarray. The size of the node correlates to an increase in the relative amount of MHC-II at the surface, an mDC-like phenotype [34, 35]. This feature was deduced from the microscopic analysis (Table S4, see Chapter 2 of this thesis). Candidate genes grouped in the same branch of the diagram, due to similar phenotypes generated, were postulated to act in the same functional pathways. We set an arbitrary threshold to distinguish four highly homologous clusters in our tree diagram (distance to root ≥153.6, genes per cluster ≥15, indicated by blue lines in Figure 4C, see also Figure S5 in Chapter 2 of this thesis). These clusters included also unknown proteins that might be functionally connected to known proteins present in the same cluster. These connections may be better understood after in-depth experimental validation.

To understand the function of the identified clusters, we determined the enrichment of Gene Ontology (GO) terms. As expected, all candidates identified by the screens were enriched for the GO cellular component term 'MHC-II protein complex' (p=0.0028815, Table S5, see Chapter 2 of this thesis). For a more extensive analyses, we applied the integrated functional gene network program Humannet v. 1 [36] that combines information from several expression and protein-protein interaction databases. We first measured the degree of connectivity between our candidates by the Area Under the Receiver Operating Characteristic (ROC) Curve (AUC) (Figure S6, see Chapter 2 of this thesis).

The AUC of 0.6175 indicates that many connected genes (neighbours) also genuinely interact. Neighbours with a log-likelihood score ≥1 according to Humannet and a |z| ≥1.645 (p<0.1) in our original flow cytometry screen were also included in this analysis (Table S6, see Chapter 2 of this thesis). These increased the number of proteins involved in the same functional pathway. Subsequent GO analysis of the expanded groups indicated that clusters 2 and 4 (Figure 4C) were enriched for 'MHC-II protein complex' (Table S5, see Chapter 2 of this thesis). When we combined this information with the microscopy phenotypes we noted that the genes in cluster 4 did not affect MHC-II distribution while those in cluster 2 showed MHC-II redistribution to the cell surface which resembles an mDC phenotype (Figure 6A). Cluster 2 has two areas where the genes cohered (Figure 5A), one was enriched for GO terms like 'MHC-II protein complex' (Figure 5B) and another for 'cytosolic ribosome' terms [cells with reduced intracellular MHC-II; (data not shown)].

The definition of clusters combined with functional annotation predicts connections between candidates within a network. This allows the addition of genes to these networks, which were not originally identified in our siRNA screen (for reasons of functional redundancy, effect below cut-off etc.). Our integrative bioinformatic approach enables us to select candidates for further biochemical studies based on their predicted functional relationships and effects observed in our various screens.

Six Proteins involved in MHC-II Redistribution in maturing DCs

To test whether our networks indeed predict processes essential in the immune system, we studied MHC-II distribution in DCs. DCs exposed to maturation signals redistribute MHC-II molecules and various activation markers from CD63-positive vesicles to the plasma membrane, enhancing their surface expression. This is an essential step in the acceleration of immune responses [34, 35] (Figure 6A). MHC-II distribution is visualized in a co-localisation pixel plot of CD63 versus MHC-II (Figure 6A, right panel). To select candidates potentially involved in the control of MHC-II redistribution in DCs, we used the following arguments. Firstly, the

A

B
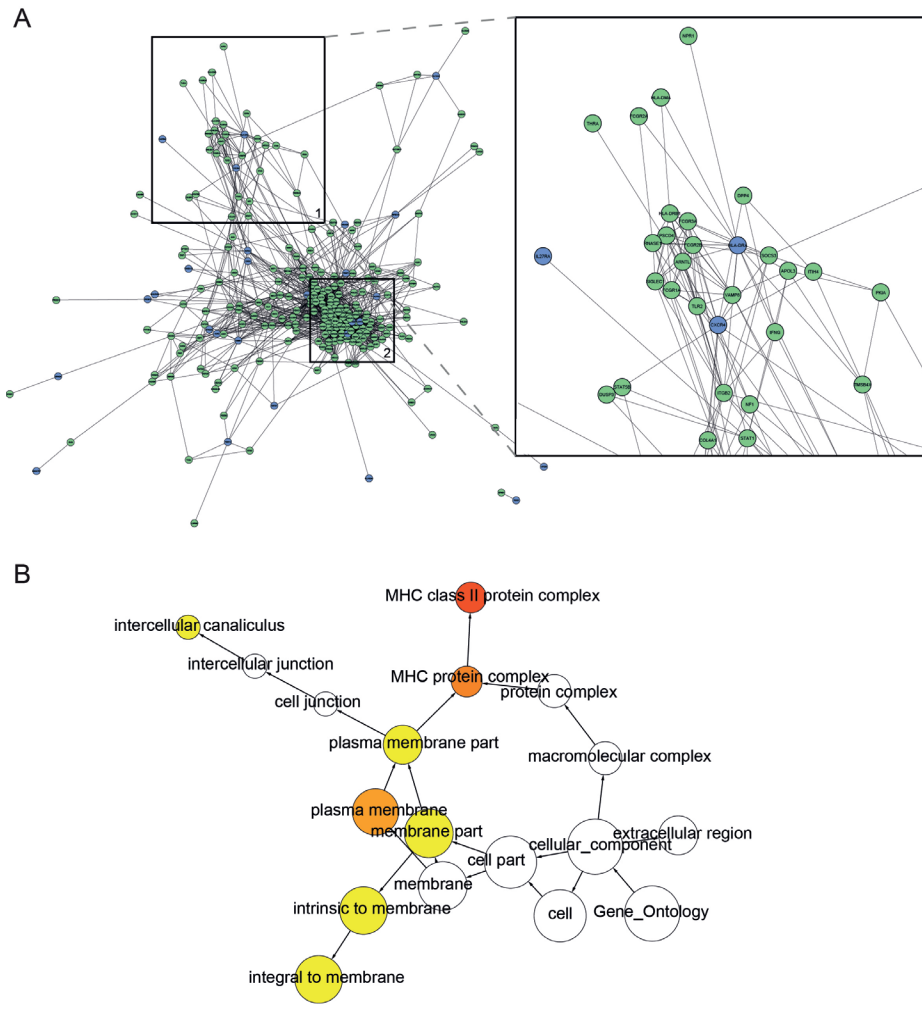
Figure 5 | MHC-II Distribution Control: Systems Analysis of Biological Pathways
A | Interaction network of genes from cluster 2 (Figure 4C). green: high scoring neighbours with |z|≥1.645 (p=0.1)
in the original flow cytometry screen, blue: genes from cluster 2. Zoom in on Box 1 is shown.
B | Gene Ontology analysis of cellular components from the aggregated genes in Box 1. The colours represent
enrichment for specific GO term (yellow to red: enriched).
See also Figure S6 and Table S5 and S6 in Chapter 2 of this thesis.

genes should up-regulate MHC-II expression at the cell surface (as in mDCs). Secondly, if upregulation is caused by silencing, the candidate should be downregulated in the microarray analyses from imDC to mDC. Lastly, silencing of genes should induce MHC-II transport to the plasma membrane as determined by microscopy (Figure 4C, Table S1, S2, see Chapter 2 of this thesis). Nine unrelated candidates fulfilled all criteria and we tested whether silencing these genes in imDCs could mimic

the reduction in expression following activation and therefore alter the distribution of MHC-II (Figure 6B). Four individual shRNA sequences per gene were introduced into primary human monocytes, before differentiation into imDCs, detected by decreased monocyte marker CD14 and increased DC marker DC-SIGN expression. Typical activation markers for mDCs remained absent (Figure 6C). Seven out of nine selected candidates increased CerCLIP and/or MHC-II expression in imDCs six days after shRNA
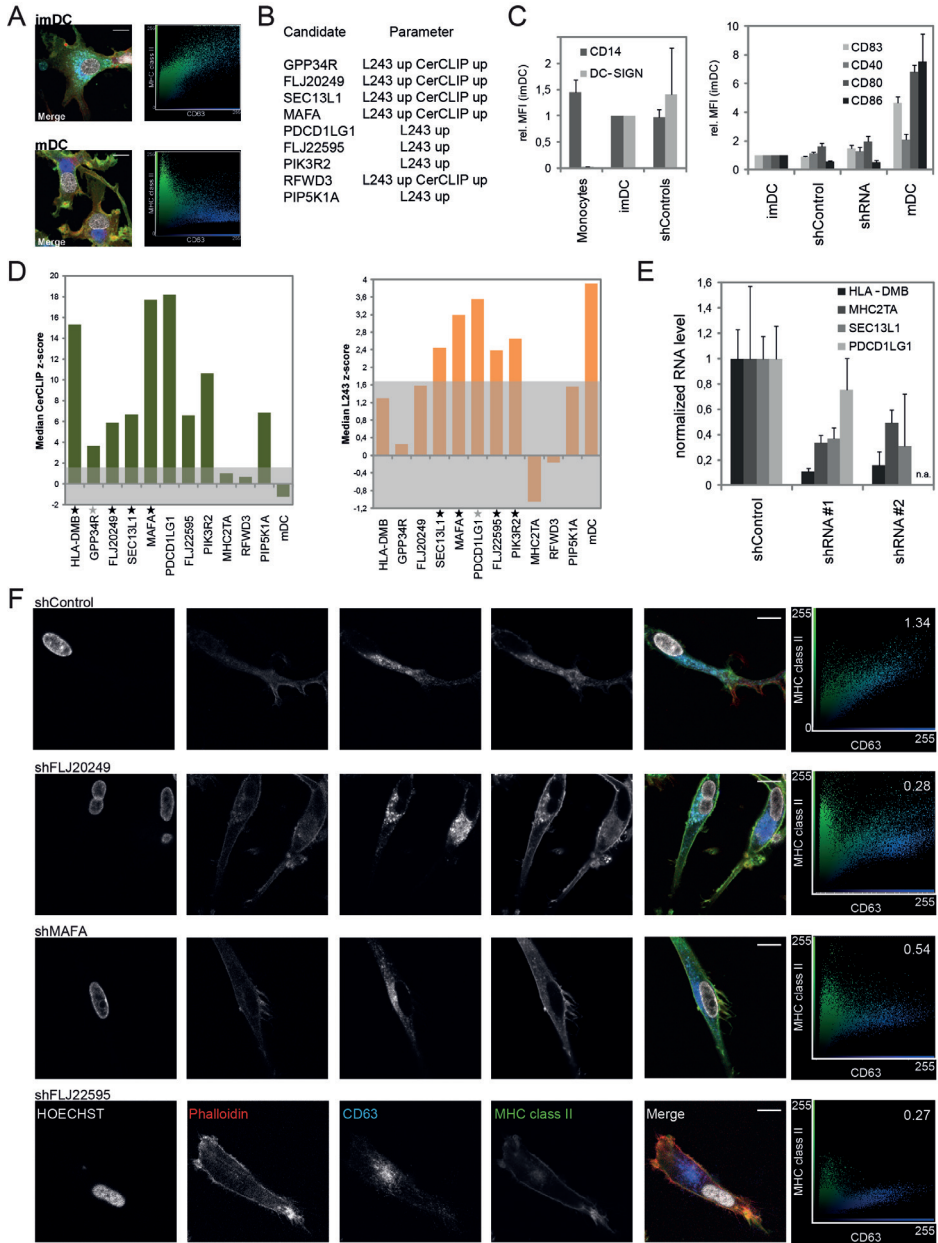
Figure 6 | MHC-II Redistribution in imDCs

A, F | Immature (imDCs) and maturated (mDCs) DCs (A) or manipulated imDCs (F) were stained for MHC-II (green), CD63 (blue), actin (phalloidin; red) and nucleus (Hoechst; white) and analyzed by confocal microscopy. Shown is the merge and the colocalisation plot per pixel for CD63 versus MHC-II (right panel) with the normalized correlation coefficient indicated (bar = 10 μm).

B | Selected candidate genes with primary screen phenotype (Table S2 in Chapter 2 of this thesis) are indicated.

C | Cell surface expression levels of monocyte (CD14), DC (DC-SIGN) and maturation markers (CD83, CD40, CD80, CD86) are plotted as averages of three donors plus standard deviation relative to levels on imDC. Four individual shRNA control vectors (shControl) or shRNAs targeting various candidate genes (shRNA) have been averaged.

Figure 6 | continued

D | Median z-score of three donors in flow cytometry after silencing candidates in imDCs plotted for one representative shRNA construct per gene. The grey box highlights the cut-off. Stars indicate confirmation of phenotype as observed in MelJuSo cells (black confirmation by >1 shRNA constructs, grey by one shRNA construct).

E | Knockdown levels determined by qPCR represented as normalized RNA levels relative to control shRNA treated cells of one donor. Two representative constructs are shown per gene. Averages plus standard deviations are plotted. n.a. not analyzed

F | Representative microscopy images of three confirmed candidates silenced by lentiviral shRNA in imDC with intracellular effects on MHC-II redistribution. The colocalisation coefficient was normalized to control shRNA-treated cells and determined by Cell Profiler. (bar = 10mm).

See also Figure S7 in Chapter 2 of this thesis.

transduction of monocytes (Figure 6D and S7A, see Chapter 2 of this thesis), similar to the effects in the primary screen. As controls, we silenced CIITA and DM, obtaining the anticipated effects on L243 and CerCLIP levels, respectively. Gene silencing was confirmed by qPCR for representative shRNA constructs (Figure 6E).

Next, the effect of silencing the nine candidates on the distribution of MHC-II in imDCs was studied by confocal microscopy. A gallery of representative images is shown in Figure S7B in Chapter 2 of this thesis. Six candidates showed a significant redistribution of MHC-II from CD63-positive compartments to the plasma membrane, which mimics the distribution of MHC-II in mDCs (Figure 6F and S7C, see Chapter 2 of this thesis). Silencing of undefined proteins FLJ20249 (GPATCH4) and FLJ22595 (the small GTPase ARL14/ARF7) as well as the transcription factor MAFA strongly affected localisation. Redistribution of MHC-II was also observed for coat protein complex II protein SEC13L1 (SEC13), Golgi protein GOLPH3-like GPP34R and PDCD1LG1 (CD274), a molecule widely expressed on immune cells involved in the regulation of T cell responses.

Our strategy identified proteins controlling MHC-II transport in imDC that would not have been selected without an unbiased approach. Silencing these genes generated imDCs with an mDC-like MHC-II distribution. These proteins control one of the strongest specific responses in the immune system and therefore open up points to target manipulation strategies at.

A Pathway of the GTPase ARL14/ARF7 and actin-based Motor Myosin 1E controls MHC-II Transport in DC

We defined various proteins controlling MHC-II transport in DCs. One of these, the GTPase ARL14/ARF7 was detected on MHC-II vesicles in imDCs (Figure 7A) and selected as a starting point for building a pathway aimed at understanding the molecular basis of MHC-II transport in DCs. Guanine

Exchange Factors (GEFs) activating ARF GTPases are specified by SEC7 domains [37]. We scanned the dataset of the primary screen (Figure 1) for proteins containing SEC7 domains that upregulated MHC-II expression, similar to ARL14/ARF7. Two candidate GEFs were identified. Their SEC7 domains were expressed as MBP-tagged proteins for *in vitro* GTP loading assays of GST-ARL14/ARF7 and GST-ARF6 as control. Only PSD4/EFA6B/TIC (selectively expressed in the immune system, z=2.22 in RNAi screen) promoted GTP loading of ARF6, as described [38] and ARL14/ARF7 (Figure 7B). The PH-domain of PSD4 was produced as GST-fusion protein and used in a lipid-binding assay which indicated specificity for various PIP2 species (Figure 7C). The candidates for controlling MHC-II transport in DC (Figure 6B) also included a regulatory subunit of PI3K (PIK3R2) [39] and PIP5K1A, which can generate PIP2. Overexpressed GFP-PIP5K1A localized to the plasma membrane and partly colocalized with intracellular MHC-II and ARL14/ARF7-mCherry vesicles in MelJuSo cells (Figure 7D) and phagosomes [40]. Collectively, this reveals part of a pathway where PIP5K1A and PIK3R2 create PIPs required for recruitment or activation of the GEF PSD4 which activates ARL14/ARF7.

GTPases require effectors to transmit function. We performed Yeast Two-Hybrid with ARL14/ARF7 as bait to identify C11ORF46 (now called ARF7 Effector Protein or ARF7EP) (Table S7, see Chapter 2 of this thesis). This 29 kDa protein does not have any detectable domains and is selectively expressed in the immune system. The interaction was confirmed by isolating ARL14/ARF7 with ARF7EP from lysates of MelJuSo expressing HA-ARF7EP and RFP-ARL14/ARF7 (Figure 7E). Immunostaining of MelJuSo cells expressing both proteins confirmed co-localization of ARL14/ARF7 and ARF7EP (Figure 7F).

Since ARF7EP does not provide any structural information that connects it to a biological pathway, we performed pull-down experiments with GST or GST-ARF7EP in cytosolic extracts of human PBMCs. Proteins found in the GST-ARF7EP isolate
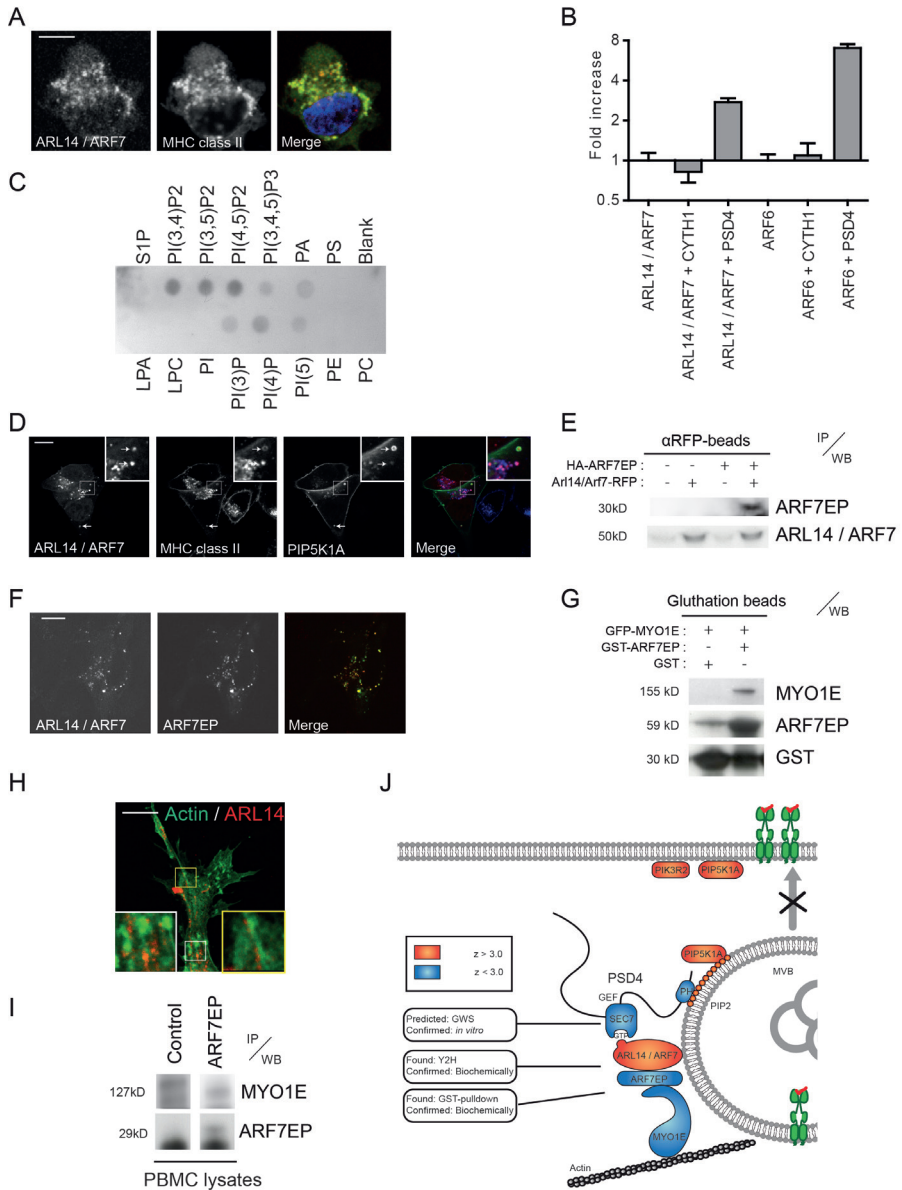
Figure 7 | Data-based Systems Determination of PIP5K-ARL14-MYO1E Pathway of MHC-II transport Control in imDC

A | Immature human monocyte-derived DCs were fixed and stained for nucleus (blue), MHC-II (green) and ARL14/ ARF7 (2C8, red). (bar = 10 mm)

B | In vitro a32P-GTP loading of ARL14/ARF7 and ARF6 by SEC7 domains of predicted GEFs CYTH1 and PSD4. Results are normalized to spontaneous loading of the two GTPases. Shown are average and standard deviation of triplicate experiments.

C | Phospholipids spotted on a membrane were probed with the GST-purified PH domain of PSD4.

D | MelJuSo cells were transfected with ARL14/ARF7-RFP and GFP-PIP5K1A, fixed and stained for MHC-II. Arrows indicate colocalisation on vesicles. (bar = 10 mm)

Figure 7 | continued

E | Immunoprecipitation (IP) of ARL14/ARF7-RFP and HA-ARF7EP expressed in MelJuSo with anti-RFP. Immunoblots were probed with HA and ARL14.2 antibodies. Molecular weight standard is indicated. See also Table S7 in Chapter 2 of this thesis.

F | Immunofluorescence of MelJuSo expressing ARL14/ARF7-RFP and GFP-ARF7EP methanol-fixed and stained with ARF7EP antibody. (bar = 10 mm)

G | Pull-down of GFP-MYO1E expressed in HEK293T with recombinant GST-ARF7EP or GST (control) coupled to Glutathione beads. Immunoblots were probed with GST and GFP antibodies. Molecular weight standard is indicated.

H | imDC stained for endogenous actin and ARL14/ARF7 (ARL14.2). Two zoom-ins are shown. (bar = 10 mm).

I | IP of endogenous ARF7EP and MYO1E in human PBMC with anti-ARF7EP or anti-GFP (Control). Immunoblots were probed with MYO1E and ARF7EP antibodies. Molecular weight standard is indicated.

J | Summarized pathway of actin-based control of MHC-II in imDC. Red proteins; candidates from the screen with |z|>3; Blue proteins with |z|<3. Identification and confirmation of the various proteins is indicated. PI kinases create substrates for the GEF PSD4 required for ARL14/ARF7 activation. The effector ARF7EP and MYO1E connect to actin.

were identified by mass spectrometry as B-actin and actin-based motor protein myosin 1E (MYO1E). Pull–down experiments from HEK293T extracts showed specific recovery of GFP-tagged MYO1E by GST-tagged ARF7EP (Figure 7G). MYO1E is a single-headed actin-based motor highly expressed in the immune system. ARL14/ARF7 may connect to the actin network via ARF7EP-MYO1E to control export of MHC-II. To test this connection, human imDC were stained with anti-actin and anti-ARL14/ARF7 antibodies (Figure 7H) revealing ARL14/ARF7 containing vesicles aligning with actin cables. The interaction between ARF7EP and MYO1E was further confirmed by immune precipitation from extracts of human PBMC (Figure 7I).

Various assays were integrated with the results of the RNAi screen to place proteins in one immune specific pathway of actin-based control of MHC-II transport in imDC (Figure 7J). Manipulation of this pathway in imDCs to induce the characteristic MHC-II transport from intracellular stores to the plasma membrane could be the result of inactivation of the ARF7GEF PSD4 by changed behavior of PI3 and PI5 kinases. How these events are controlled in DCs during activation is unknown. By extensive dataset integration, we defined a pathway controlling one of the most essential steps in immune cell activation; the redistribution of MHC-II to the plasma membrane in DCs after maturation.

Discussion

We describe here the genome-wide analysis of an essential process in the immune system: antigen presentation by MHC-II. We identify 276 candidates with only 10% described thus far in the MHC-II pathway. Twenty-one candidates are linked to autoimmune diseases. As in our siRNA experiments, these genes may cause aberrant MHC-II expression

in patients, which requires further experimental validation before consideration for therapeutic manipulation.

We have developed various methods to place the candidate genes in the systems of transcriptional and cell biological control of MHC-II antigen presentation. By flow cytometry we selected 45 genes affecting peptide loading only, including HLA-DM and components of the ESCRT machinery involved in multivesicular body formation. A limited set of genes could be placed in networks by computer-based pathway analysis, unlike the majority of genes, which have an unknown function. This represents an enigma in high-throughput screening yielding large datasets and often results in preselecting one gene for in-depth analysis with limited new understanding of biology.

There are two important unelucidated processes in MHC-II antigen presentation, which we addressed in our study in detail: the control of tissue specific expression of MHC-II and the regulation of MHC-II distribution in DCs. MHC-II expression is controlled by CIITA. How CIITA in turn is regulated is unclear. We discovered nine transcriptional regulators of MHC-II expression and performed cross-correlative qPCR to determine their interrelationships and their effects on CIITA expression. Five of these regulate the expression levels of CIITA in a complex feedback loop involving the (yeast meiosis) factor RMND5B and MAPK1 that phosphorylates and influences CIITA activity [41]. The remaining factors control MHC-II expression without affecting CIITA levels. This includes the HIV Tat interacting protein HTATIP, a histone modifier that may mediate Tat control of MHC-II expression [25, 42]. By combining experimental and literature data, we show that the activities of extracellular signalling, the cell cycle and chromatin modifications control the transcriptional network for immune tissue-restricted MHC-II expression. Of note, pathogens also

manipulate these pathways; HIV targets HTATIP and *L. monocytogenes* targets SMAD4 [25, 43]. Tissue selective expression of MHC-II is thus orchestrated by a series of unrelated input signals. The details of how these cooperate to induce proper MHC-II expression remain unclear.

To identify proteins controlling MHC-II distribution, we silenced all candidates and the effect on MHC-II distribution was visualized by microscopy. Candidate genes inducing a similar phenotype are expected to participate in one network, as illustrated in yeast screens that identified the ESCRT machinery [44]. We integrated our phenotypic clusters with databases like Humannet v. 1 to expand our networks and annotated these using GO analyses. Half of the genes in these clusters were predicted to control MHC-II trafficking but will require further experiments to validate their place in networks.

To select candidates involved in MHC-II redistribution in DCs, expression and functional RNAi datasets were combined to define six proteins controlling MHC-II transport. Silencing these resulted in imDCs with an mDC-like MHC-II distribution. These six candidates could act in one or parallel pathways.

One candidate, ARL14/ARF7, is a GTPase selectively expressed in immune cells. To build a pathway, we first localized ARL14/ARF7 on MHC-II compartments in imDC. Using domain predictions and *in vitro* assays, we defined the GEF for ARL14/ARF7 as PSD4. PSD4 contains a PH-domain with specificity for various PIP2 species which may result from activities of two other proteins proposed to control MHC-II distribution in DCs: PIK3R2 and PIP5K1A. While PI(3,5)P2 locates to late endosomes [45], the PH-domain of PSD4 has a broader specificity and can therefore not induce selective targeting of PSD4 to late endosomes. The 60 kDa N-terminal domain of PSD4 may induce targeting to endosomal vesicles [38]. When detecting PIP2, the PH domain of PSD4 might position the preceding SEC7 domain correctly for supporting GTP loading of ARL14/ARF7. To further expand the network, an interaction of the ARL14/ARF7 effector ARF7EP with the actin-based motor MYO1E was defined. This pathway connects general signalling events to actin-based transport control of MHC-II compartments in DCs.

While PIK3R2 and PIP5K1A upstream are broadly expressed proteins, the other proteins in this pathway are more immune system selective. Of note, another candidate for controlling MHC-II distribution in DCs, PDCD1LG1 (CD274, PD-L1) activates PI3K via its receptor PD-1. PD-1 delivers inhibitory signals regulating T cell activation and tolerance. Little is known about PD-L1 signalling [46] and this signalling may be irrelevant in mDC [47]. Tissue selective control of actin-based transport by GTPases has been shown before for melanosomes where GTPase

RAB27a binds MYO5A via its effector Melanophylin [48]. MYO1E may be involved in granule secretion [49] as well as endocytosis by coupling to dynamin [50]. MYO1E may have multiple functions in actin-based processes depending on recruitment to specific locations. We define ARL14/ARF7-ARF7EP as a MYO1E receptor on MHC-II compartments for actin-based transport control. How the previously observed interaction between another actin-based motor MYH9 and MHC-II-associated Ii contributes to this process is unclear [51].

The four remaining proteins controlling MHC-II transport in imDC could not be placed in this pathway: MAFA is a transcription factor for insulin in pancreatic beta cells [52]. Our microarray data do not show any insulin production in DCs because the transcription co-factors Pdx-1 and NeuroD1 [53] are not expressed. SEC13L1 (SEC13) is a COPII protein controlling transport between ER and Golgi [54] which is a non immune-specific process in cells. GOLPH3L might have a similar function in the Golgi as GOLPH3 [55]. The function of the fourth protein, GPATCH4 is unknown. It remains to be elucidated whether and how GPATCH4 could manipulate MHC-II antigen presentation.

We describe here a genome-wide analysis of molecules acting on a central controller in the immune system: MHC-II. After a first candidate selection by flow cytometry, we applied two additional high-throughput techniques and integrated the data with expression and protein interaction databases, cross-correlative qPCR, Yeast Two-Hybrid and proteomics. We defined a transcriptional network for MHC-II and CIITA, and a cell biological pathway placing ARL14/ARF7, its effector ARF7EP and MYO1E in control of actin-based MHC-II transport in DCs. This study identifies new targets and pathways for chemical and biological manipulation of MHC-II expression in various diseases, including autoimmunity.

Experimental Procedures

siRNA Transfection, Flow cytometry and Microarray

Gene silencing was performed in the human melanoma cell line (MelJuSo) using DharmaFECT transfection reagent #1 and 50 nM siRNA (Human siGenome SMARTpool library, Dharmacon). Three days post-transfection, cells were analyzed by flow cytometry (BD FACSArray) using L243-Cy3 [22] and CerCLIP-Cy5 [21] monoclonal antibodies. The data was normalized (cellHTS, Bioconductor) and transformed into z-scores [56]. Expression levels of genes with $|z|>3$ were determined by microarray analysis (Illumina) in primary human monocytes, DCs and B cells; isolated and differentiated as previously

described [57, 58]. Mature DCs were generated by culturing for two days in the presence of 2.5 μg/ml LPS (Invivogen) and 1000 U/ml IFNγ (Immukine, Boehringer Ingelheim).

For statistical analysis, p-values were determined using the Student's t test.

Quantitative RT-PCR

Messenger RNA was extracted (mRNA Capture Kit) and reverse transcribed into cDNA (Transcriptor High Fidelity cDNA Synthesis Kit). The quantitative RT-PCR was performed using LightCycler® 480 SYBR Green 1 Master on the LightCycler® 480 Detection System (all Roche). Quantification was performed using the comparative CT method (ΔΔCT). Primer sequences are available upon request.

Confocal Microscopy

Distribution of MHC-II, early endosomes and Golgi was visualized by confocal microscopy (Leica AOBS microscope) using MelJuSo stably expressing HLA-DRB1-GFP, mCherry-GalT2 and stained with anti-EEA1 (BD transduction laboratories) and Hoechst (Invitrogen). DCs were stained using Hoechst, Phalloidin-Alexa568 (Molecular Probes), anti-ARL14 2C8 (BioConnect), anti-CD63 (NKI-C3) and anti-HLA-DR [3]. Images were analyzed using CellProfiler 1.0.5811 [32]. CPAnalyst 2 was used to determine the minimal set of parameters needed to describe the relevant phenotypes [33]. The "Measure Correlation" module of CellProfiler was used to determine the correlation between CD63 and MHC-II. MelJuSo cells were cultured with 3 ng/ml TGFβ for three days. Cells were stained with anti-SMAD4 (Santa Cruz) and anti-RMND5B (Abcam) antibodies. Open and proprietary software was used for pathway analysis as described extensively in the Supplemental Experimental Procedures.

DC Manipulation

Human primary monocytes were transduced with lentiviral particles in the presence of 4 μg/ml polybrene (Millipore) at a MOI of 2. Viruses were produced by 293T cells transfected with packaging (pRSVrev, pHCMV-G VSV-G, pMDLg/pRRE) and pLKO.1shRNA constructs (Open Biosystems, Thermo Scientific) using Fugene 6 (Roche). Monocytes were subsequently cultured for six days in the presence of 800 U/ml IL-4 and 1,000 U/ml GM-CSF (Cellgenix) to generate imDCs. DC cell surface marker levels were determined by flow cytometry after staining with the following mouse anti-human antibodies: FITC CD14, APC DC-SIGN, PE HLA-DR (L243), FITC CD83, APC CD40, PE CD80, APC CD86 (all from BD).

Pathway building Techniques

Yeast Two-Hybrid was performed at DKFZ (Heidelberg) with ARL14-Q68L without myristoylation site cloned in pGBT9. ARF7EP was cloned in a bacterial expression vector as a GST-chimera and purified. Recombinant GST-ARF7EP and GST as a control were used to fish for endogenous MYO1E from cytosolic extracts of human PBMCs and bound fractions were analyzed by mass spectrometry. Biochemical GEF assays were performed with purified MBP-tagged SEC7 domains from CYTH1 and PSD4 and GST-purified ARL14 or ARF6 using a32P-GTP. The PH domain of PSD4 was isolated as a GST-PHPH protein from 293T cells and used to probe phospholipid membranes (tebu-bio). For antibodies used to immune precipitate see Supplemental Experimental Procedures in Chapter 2 of this thesis.

1

References

1. Reith, W., S. LeibundGut-Landmann, and J.M. Waldburger, *Regulation of MHC class II gene expression by the class II transactivator.* Nat.Rev. Immunol., 2005. **5**(10): p. 793-806.

2. Chaplin, D.D. and M.E. Kemp, *The major histocompatibility complex and autoimmunity.* Year.Immunol, 1988. **3**: p. 179-198.

3. Neefjes, J.J., et al., *The biosynthetic pathway of MHC class II but not class I molecules intersects the endocytic route.* Cell, 1990. **61**(1): p. 171-183.

4. Roche, P.A. and P. Cresswell, *Invariant chain association with HLA-DR molecules inhibits immunogenic peptide binding.* Nature, 1990. **345**(6276): p. 615-618.

5. Riberdy, J.M., et al., *HLA-DR molecules from an antigen-processing mutant cell line are associated with invariant chain peptides.* Nature, 1992. **360**(6403): p. 474-477.

6. Denzin, L.K., C. Hammond, and P. Cresswell, *HLA-DM interactions with intermediates in HLA-DR maturation and a role for HLA-DM in stabilizing empty HLA-DR molecules.* J.Exp.Med., 1996. **184**(6): p. 2153-2165.

7. Sloan, V.S., et al., *Mediation by HLA-DM of dissociation of peptides from HLA-DR.* Nature, 1995. **375**(6534): p. 802-806.

8. Zwart, W., et al., *Spatial separation of HLA-DM/HLA-DR interactions within MIIC and phagosome-induced immune escape.* Immunity, 2005. **22**(2): p. 221-233.

9. Boes, M., et al., *T-cell engagement of dendritic cells rapidly rearranges MHC class II transport.* Nature, 2002. **418**(6901): p. 983-988.

10. Chow, A., et al., *Dendritic cell maturation triggers retrograde MHC class II transport from lysosomes to the plasma membrane.* Nature, 2002. **418**(6901): p. 988-994.

11. Wubbolts, R., et al., *Direct vesicular transport of MHC class II molecules from lysosomal structures to the cell surface.* J.Cell Biol., 1996. **135**(3): p. 611-622.

12. Koppelman, B., et al., *Interleukin-10 down-regulates MHC class II alphabeta peptide complexes at the plasma membrane of monocytes by affecting arrival and recycling.* Immunity, 1997. **7**(6): p. 861-871.

13. Steimle, V., et al., *Regulation of MHC class II expression by interferon-gamma mediated by the transactivator gene CIITA.* Science, 1994. **265**(5168): p. 106-109.

14. Blander, J.M. and R. Medzhitov, *Toll-dependent selection of microbial antigens for presentation by dendritic cells.* Nature, 2006. **440**(7085): p. 808-812.

15. Thibodeau, J., et al., *Interleukin-10-induced MARCH1 mediates intracellular sequestration of MHC class II in monocytes.* Eur J Immunol, 2008. **38**(5): p. 1225-1230.

16. Ziegler, H.K. and E.R. Unanue, *Decrease in macrophage antigen catabolism caused by ammonia and chloroquine is associated with inhibition of antigen presentation to T cells.* Proc. Natl.Acad.Sci.U S A, 1982. **79**(1): p. 175-178.

17. Anderson, H.A. and P.A. Roche, *Phosphorylation regulates the delivery of MHC class II invariant chain complexes to antigen processing compartments.* J.Immunol., 1998. **160**(10): p. 4850-4858.

18. Kuipers, H.F., et al., *Statins affect cell-surface expression of major histocompatibility complex class II molecules by disrupting cholesterol-containing microdomains.* Hum.Immunol., 2005. **66**(6): p. 653-665.

19. Agrawal, S. and E.R. Kandimalla, *Role of Toll-like receptors in antisense and siRNA [corrected].* Nat Biotechnol, 2004. **22**(12): p. 1533-1537.

20. Reynolds, A., et al., *Induction of the interferon response by siRNA is cell type- and duplex length-dependent.* RNA., 2006. **12**(6): p. 988-993.

21. Denzin, L.K., et al., *Assembly and intracellular transport of HLA-DM and correction of the class II antigen-processing defect in T2 cells.* Immunity, 1994. **1**(7): p. 595-606.

22. Lampson, L.A. and R. Levy, *Two populations of Ia-like molecules on a human B cell line.* J.Immunol., 1980. **125**(1): p. 293-299.

23. Zhang, J.H., T.D. Chung, and K.R. Oldenburg, *A Simple Statistical Parameter for Use in Evaluation and Validation of High Throughput Screening Assays.* J Biomol Screen, 1999. **4**(2): p. 67-73.

24. Imai, A., et al., *Inhibition of endogenous MHC class II-restricted antigen presentation by tacrolimus (FK506) via FKBP51.* Eur J Immunol, 2007. **37**(7): p. 1730-1738.

25. Kamine, J., et al., *Identification of a cellular protein that specifically interacts with the essential cysteine region of the HIV-1 Tat transactivator.* Virology, 1996. **216**(2): p. 357-366.

26. Wu, C., et al., *BioGPS: an extensible and customizable portal for querying and organizing gene annotation resources.* Genome Biol, 2009. **10**(11): p. R130.

27. Snel, B., et al., *STRING: a web-server to retrieve and display the repeatedly occurring neighbourhood of a gene.* Nucleic Acids Res, 2000. **28**(18): p. 3442-3444.

28. Horton, R., et al., *Gene map of the extended human MHC.* Nat Rev Genet, 2004. **5**(12): p. 889-899.

29. Colland, F., et al., *Functional proteomics mapping of a human signaling pathway.* Genome Res, 2004. **14**(7): p. 1324-1332.

30. Dong, Y., et al., *The Smad3 protein is involved in TGF-beta inhibition of class II transactivator and class II MHC expression.* J Immunol, 2001. **167**(1): p. 311-319.

31. Shi, Y. and J. Massague, *Mechanisms of TGF-beta signaling from cell membrane to the nucleus.* Cell, 2003. **113**(6): p. 685-700.

32. Carpenter, A., et al., *CellProfiler: image analysis software for identifying and quantifying cell phenotypes.* Genome Biology, 2006. **7**(10): p. R100.

33. Jones, T.R., et al., *Scoring diverse cellular morphologies in image-based screens with iterative feedback and machine learning.* Proc Natl Acad Sci U S A, 2009. **106**(6): p. 1826-1831.

34. Cella, M., et al., *Inflammatory stimuli induce accumulation of MHC class II complexes on dendritic cells.* Nature, 1997. **388**(6644): p. 782-787.

35. Pierre, P., et al., *Developmental regulation of MHC class II transport in mouse dendritic cells.* Nature, 1997. **388**(6644): p. 787-792.

36. Kim, W.K., C. Krumpelman, and E.M. Marcotte, *Inferring mouse gene functions from genomic-scale data using a combined functional network/classification strategy.* Genome Biol, 2008. **9 Suppl 1**: p. S5.

37. Casanova, J.E., *Regulation of Arf activation: the Sec7 family of guanine nucleotide exchange factors.* Traffic, 2007. **8**(11): p. 1476-1485.

38. Derrien, V., et al., *A conserved C-terminal domain of EFA6-family ARF6-guanine nucleotide exchange factors induces lengthening of microvilli-like membrane protrusions.* J Cell Sci, 2002. **115**(Pt 14): p. 2867-2879.

39. Deane, J.A. and D.A. Fruman, *Phosphoinositide 3-kinase: diverse roles in immune cell activation.* Annu Rev Immunol, 2004. **22**: p. 563-598.

40. Mao, Y.S., et al., *Essential and unique roles of PIP5K-gamma and -alpha in Fcgamma receptor-mediated phagocytosis.* J Cell Biol, 2009. **184**(2): p. 281-296.

41. Voong, L.N., et al., *Mitogen-activated protein kinase ERK1/2 regulates the class II transactivator.* J.Biol.Chem., 2008. **283**(14): p. 9031-9039.

42. Kanazawa, S., T. Okamoto, and B.M. Peterlin, *Tat competes with CIITA for the binding to P-TEFb and blocks the expression of MHC class II genes in HIV infection.* Immunity, 2000. **12**(1): p. 61-70.

43. Ribet, D., et al., *Listeria monocytogenes impairs SUMOylation for efficient infection.* Nature, 2010. **464**(7292): p. 1192-1195.

44. Teis, D., S. Saksena, and S.D. Emr, *Ordered assembly of the ESCRT-III complex on endosomes is required to sequester cargo during MVB formation.* Dev Cell, 2008. **15**(4): p. 578-589.

45. Vicinanza, M., et al., *Function and dysfunction of the PI system in membrane trafficking.* EMBO J, 2008. **27**(19): p. 2457-2470.

46. Keir, M.E., et al., *PD-1 and its ligands in tolerance and immunity.* Annu Rev Immunol, 2008. **26**: p. 677-704.

47. Breton, G., et al., *siRNA knockdown of PD-L1 and PD-L2 in monocyte-derived dendritic cells only modestly improves proliferative responses to Gag by CD8(+) T cells from HIV-1-infected individuals.* J Clin Immunol, 2009. **29**(5): p. 637-645.

48. Seabra, M.C. and E. Coudrier, *Rab GTPases and myosin motors in organelle motility.* Traffic, 2004. **5**(6): p. 393-399.

49. Schietroma, C., et al., *A role for myosin 1e in cortical granule exocytosis in Xenopus oocytes.* J Biol Chem, 2007. **282**(40): p. 29504-29513.

50. Krendel, M., E.K. Osterweil, and M.S. Mooseker, *Myosin 1E interacts with synaptojanin-1 and dynamin and is involved in endocytosis.* FEBS Lett, 2007. **581**(4): p. 644-650.

51. Vascotto, F., et al., *The actin-based motor protein myosin II regulates MHC class II trafficking and BCR-driven antigen presentation.* J Cell Biol, 2007. **176**(7): p. 1007-1019.

52. Olbrot, M., et al., *Identification of beta-cell-specific insulin gene transcription factor RIPE3b1 as mammalian MafA.* Proc Natl Acad Sci U S A, 2002. **99**(10): p. 6737-6742.

53. Cerf, M.E., *Transcription factors regulating beta-cell function.* Eur J Endocrinol, 2006. **155**(5): p. 671-679.

54. Tang, B.L., et al., *The mammalian homolog of yeast Sec13p is enriched in the intermediate compartment and is essential for protein transport from the endoplasmic reticulum to the Golgi apparatus.* Mol Cell Biol, 1997. **17**(1): p. 256-266.

55. Dippold, H.C., et al., *GOLPH3 bridges phosphatidylinositol-4-phosphate and actomyosin to stretch and shape the Golgi to promote budding.* Cell, 2009. **139**(2): p. 337-351.

56. Boutros, M., L.P. Bras, and W. Huber, *Analysis of cell-based RNAi screens.* Genome Biol., 2006. **7**(7): p. R66.

57. Souwer, Y., et al., *B cell receptor-mediated internalization of salmonella: a novel pathway for autonomous B cell activation and antibody production.* J Immunol, 2009. **182**(12): p. 7473-7481.

58. Ten Brinke, A., et al., *The clinical grade maturation cocktail monophosphoryl lipid A plus IFNgamma generates monocyte-derived dendritic cells with the capacity to migrate and induce Th1 polarization.* Vaccine, 2007. **25**(41): p. 7145-7152.

1